

Diurnal Variations in the Community Climate System Model

Aiguo Dai* and Kevin E. Trenberth
National Center for Atmospheric Research (NCAR)[§], Boulder, CO

Abstract

Diurnal (or sub-daily) variations are large in many surface and atmospheric fields such as solar radiation, surface latent and sensible heat fluxes, surface temperature and winds, atmospheric convection, and precipitation. These diurnal variations are especially important in air-land and air-sea interactions, which are highly non-linear and thus can not be resolved using daily mean values. Current regional and global climate models still have difficulties in simulating the diurnal variations correctly. Here we analyze the diurnal variations in surface air temperature and pressure, precipitation, and cloudiness simulated by the Community Climate System Model (CCSM), a state-of-art climate system model developed by a large number of scientists from the National Center for Atmospheric Research (NCAR) and partner institutions. The CCSM simulates well some aspects of diurnal variations such as the diurnal and semidiurnal pressure tides, and the diurnal cycle of temperature over land; but it has large biases in simulating diurnal cycles in cloud amount, moist convection, and precipitation. Diurnal variations over the oceans are too weak in the CCSM mainly because the surface ocean has no diurnal cycle in the model.

1. Introduction

In order to realistically simulate monthly to decadal mean fields of the atmosphere and oceans, climate models have to resolve the physics of the climate system on small and short time scales. This is because many of the physical processes, such as atmospheric convection, radiation, and surface evaporation, are highly non-linear and can not be represented adequately using averaged fields. One example of the high-frequency variations is the sub-daily or diurnal variations that are pronounced near the earth's surface resulting from the diurnal cycle of solar radiation. Because of the regular diurnal forcing from the Sun, the diurnal variations in a number of fields (e.g., air temperature, pressure, winds, precipitation, etc.) have preferred phase and distinct mean diurnal patterns. However, many sub-daily variations, such as those associated with wind bursts, have no preferred diurnal phase (i.e. random) and do not show up in the averaged mean diurnal cycle. Nevertheless, these random sub-

daily variations, which can be large in magnitude and last for several hours, can also have significant impacts on some physical processes such surface latent and sensible heat fluxes over the oceans (Zeng et al. 2002). It is therefore very important to resolve the near surface fields on short (e.g., hourly) time scales in climate and weather prediction models.

Most atmospheric general circulations models (AGCMs) resolve the atmospheric sub-daily variations and are coupled to a land surface model that also resolves the land surface diurnal cycle. However, most oceanic general circulations models (OGCMs) do not have a surface model that can resolve the diurnal cycle within the top 10 m or so of the oceans. As a result, the diurnal cycles in surface air and sea temperatures, surface latent and sensible heat fluxes, and other near surface fields are not simulated well in most coupled GCMs. In addition, other atmospheric processes related to the surface diurnal cycles, such as the afternoon cumulus convection associated with peak ocean skin temperatures (Sui et al. 1997; Chen and Houze 1997), are unlikely to be simulated by these coupled GCMs.

Here we examine the diurnal variability in the Community Climate System Model (CCSM) (Blackmon et al. 2001), a state-of-art climate system model developed by a large number of scientists from the National Center for Atmospheric Research (NCAR) and

* Corresponding author address: Aiguo Dai, NCAR/CGD, P.O. Box 3000, Boulder, CO 80307.

§ The National Center for Atmospheric Research is sponsored by the National Science Foundation.

partner institutions. We focus only on the mean diurnal cycles in surface air temperature, pressure, precipitation and cloudiness. Three-hourly (instantaneous) fields from a 10-yr period (yr 500-509) of a multi-century control run were averaged to derive the mean diurnal cycles, which are compared to available observations. The CCSM has a resolution of T42 ($\sim 2.8^\circ$) with 26 layers for the AGCM and $\sim 1^\circ$ nominal grid size with 40 layers for the OGCM (10 m thickness for the top layer). Because the CCSM does not have an ocean surface model and has to use the top ocean-layer temperature as the sea surface temperature (SST) for air-sea coupling, the ocean surface in the CCSM has no diurnal cycle.

This model deficiency affects the diurnal variations in many other fields (including surface air temperature) over the oceans, resulting in a generally weak diurnal cycle over the oceans in the CCSM.

2. Results

Fig.1 shows the mean diurnal anomalies (relative to long-term daily mean) of December-February (DJF) surface air temperature from surface observations and the CCSM. It can be seen that the CCSM simulates the

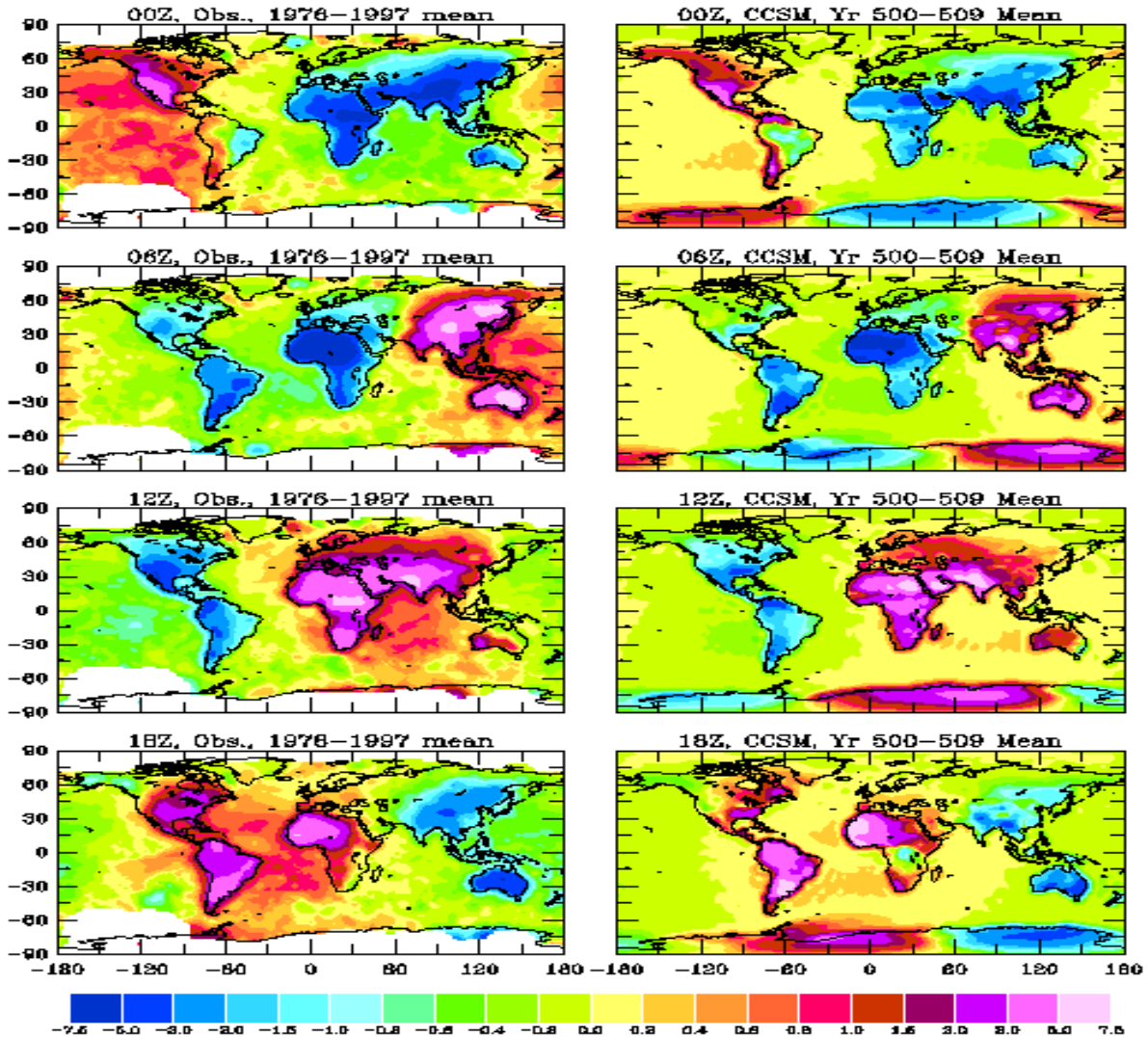


Fig. 1: Mean DJF diurnal anomalies of observed (*left*) and CCSM-simulated (*right*) surface air temperature at 0000, 0600, 1200 and 1800 UTC. The observed air temperature was derived based on synoptic observations from over 15,000 stations and from the COADS during 1976-1997. The local radiative heating effect on ship temperature records was corrected using a scheme described by Kent et al. (1993). The color scales are $\pm 0.2, 0.4, 0.6, 0.8, 1.0, 1.5, 2.0, 3.0, 5.0,$ and 7.5°C .

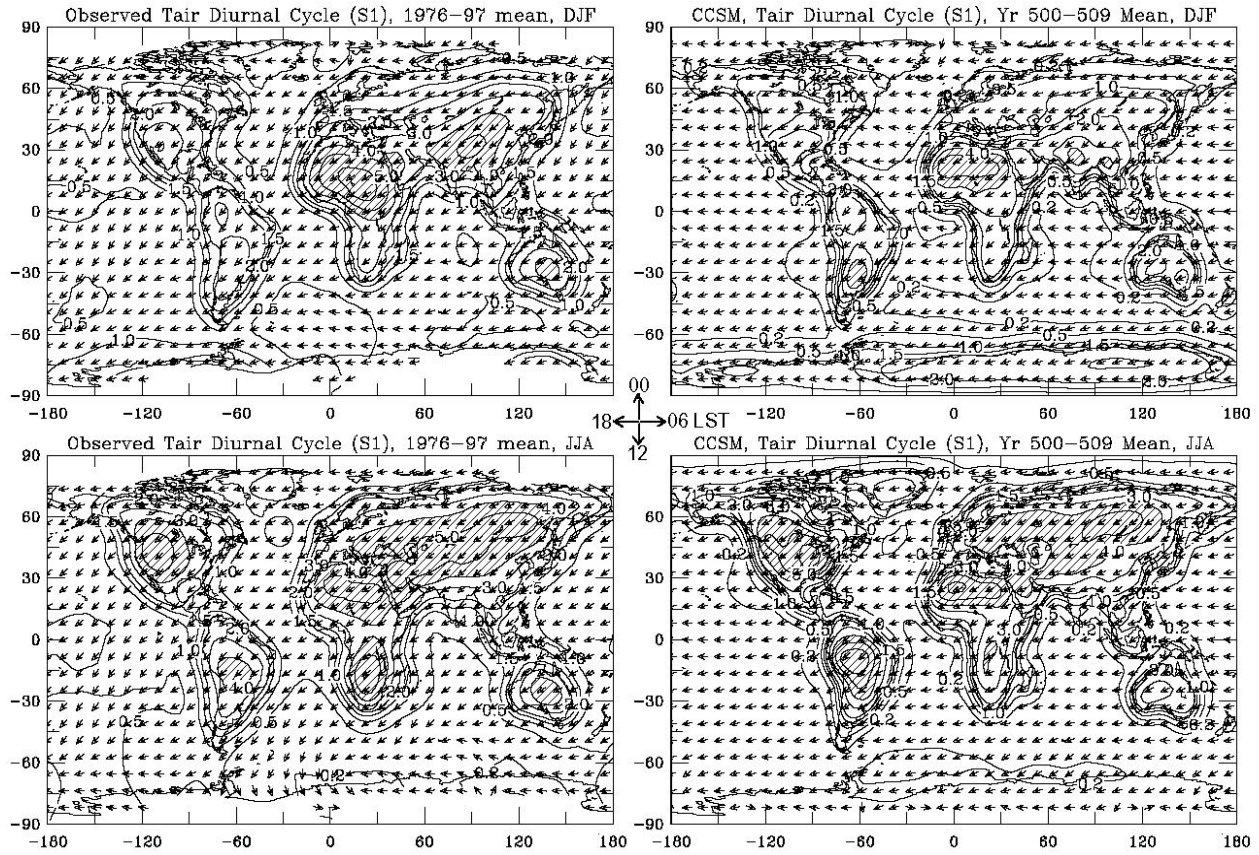


Fig. 2: Amplitude (contours, °C) and local solar time at the maximum (arrows, central phase clock) of the diurnal (24hr) harmonic of DJF (*top row*) and JJA (*bottom row*) surface air temperature from observations (*left*) and the CCSM (*right*). Contour values over 4.0 °C are hatched.

temperature anomalies over the continents quite well. For example, the large anomalies (3-8°C) over the Tibetan Plateau and the Saharan desert are captured by the CCSM. This suggests that the daytime solar heating and nighttime radiative cooling near the ground are represented well in the CCSM. On the other hand, the diurnal anomalies of air temperature over the oceans are too small in the CCSM (~0.0-0.4°C) compared with the observations (0.4-1.0°C) and the NCEP/NCAR reanalysis (not shown). As mentioned above, this weak diurnal cycle over the ocean surface results from the model deficiency to simulate the diurnal variations within the surface oceans (daily mean solar radiation and other atmospheric fields were used to force the ocean GCM in the CCSM).

Fig. 2 shows the amplitude and phase (local solar time or LST of the maximum) of the diurnal harmonic (S_1) of the temperature anomalies shown in Fig. 1 (also including June-August or JJA season). The S_1 dominates the sub-daily variation in surface air temperature and accounts for most (>80% over land)

variance. The observed S_1 peaks around 1400-1600 LST and the phase varies little land and ocean and from winter to summer. The amplitude is much larger over land (1-6°C) than over ocean (~0.5°C), and is largest over high terrain during summer. The CCSM simulates these broad features fairly well. Over the oceans, however, the amplitude in the model ($\leq 0.2^\circ\text{C}$) is too small, as pointed out above, and the phase is ~2hr late.

Another well-known sub-daily variation is the surface pressure tides. Fig. 3 shows the mean diurnal anomalies of DJF surface pressure from observations (Dai and Wang 1999) and the CCSM, which has a atmospheric top at ~2 mb. The CCSM simulates well both the regional amplitudes (up to 2 mb) and the westward propagation of the wave number 2 mode, but it overestimates the amplitudes, especially over tropical land areas (e.g., South America). Fig. 4 compares the diurnal pressure tide from observations and the CCSM. While the overall patterns (e.g., larger amplitude over land (0.4-1.4 mb) than over ocean (0.4-0.6 mb)) are simulated well, the model overestimates the diurnal

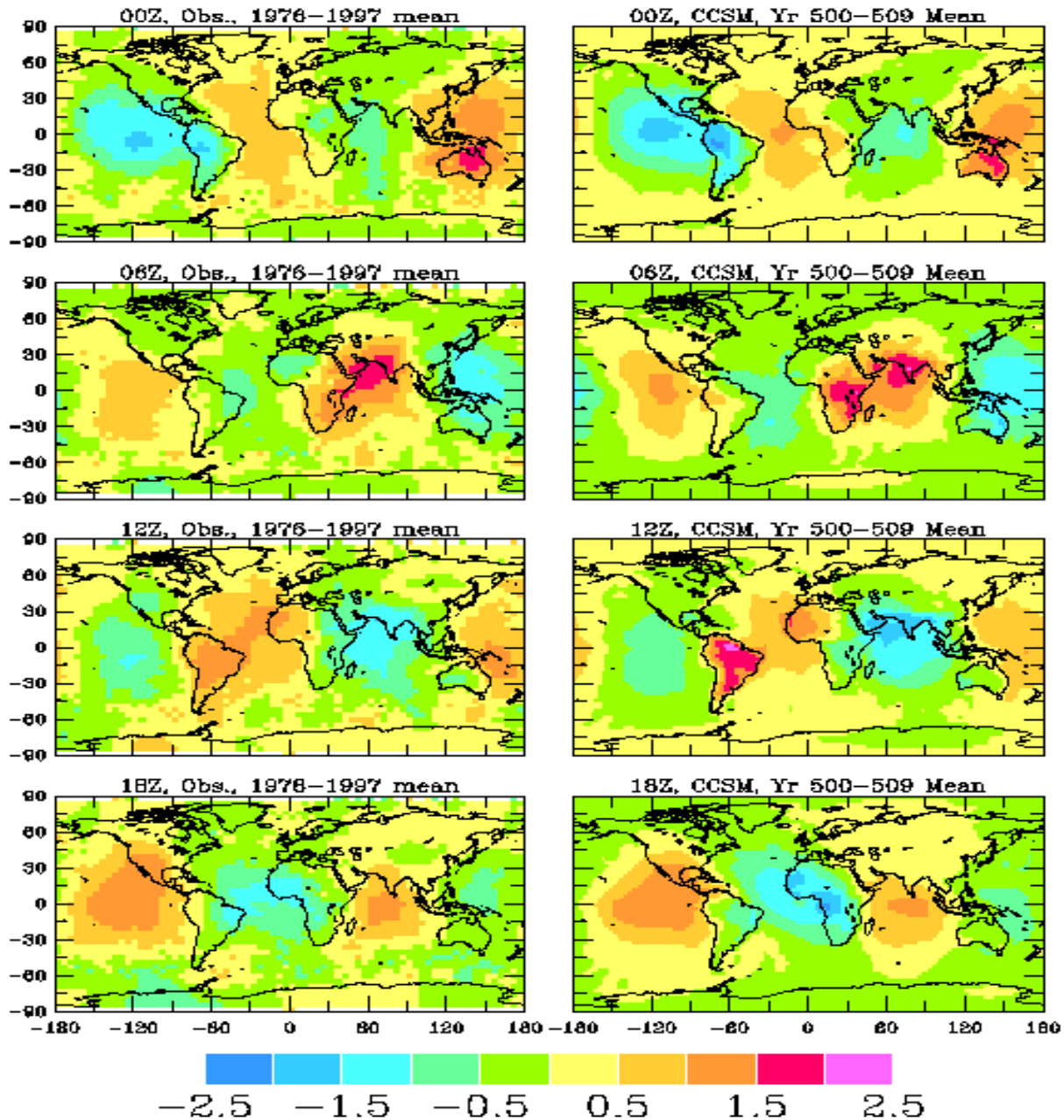


Fig. 3: Mean DJF diurnal anomalies of observed (*left*, from Dai and Wang 1999) and CCSM-simulated (*right*) surface air pressure (in mb) at 0000, 0600, 1200 and 1800 UTC.

amplitude (by 20-50%) over low-latitude land areas and underestimates it over most oceans, the Rockies and other northern mid-latitude land areas. The simulated diurnal phase agrees with the observed over most oceans and mid-latitude land areas. At low latitudes, the phase is around 0600 LST over both land and ocean in the CCSM, whereas land lags ocean by ~ 2 hr in the observations. The semidiurnal (S_2) pressure tide is simulated well by the CCSM in terms of the amplitude,

phase and the seasonal cycle (Fig.5). For example, both the observations and the CCSM show the semidiurnal pressure tide peaks around 0930-1030 LST (and 12 hrs later) with an amplitude of 0.8-1.2 mb in the latitudes (30°S - 30°N). The model-simulated S_2 amplitude is slightly smaller (especially over the eastern Pacific Ocean) and has less zonal variation than in the observations. The latter contain sampling errors that might partly contribute to the zonal variations.

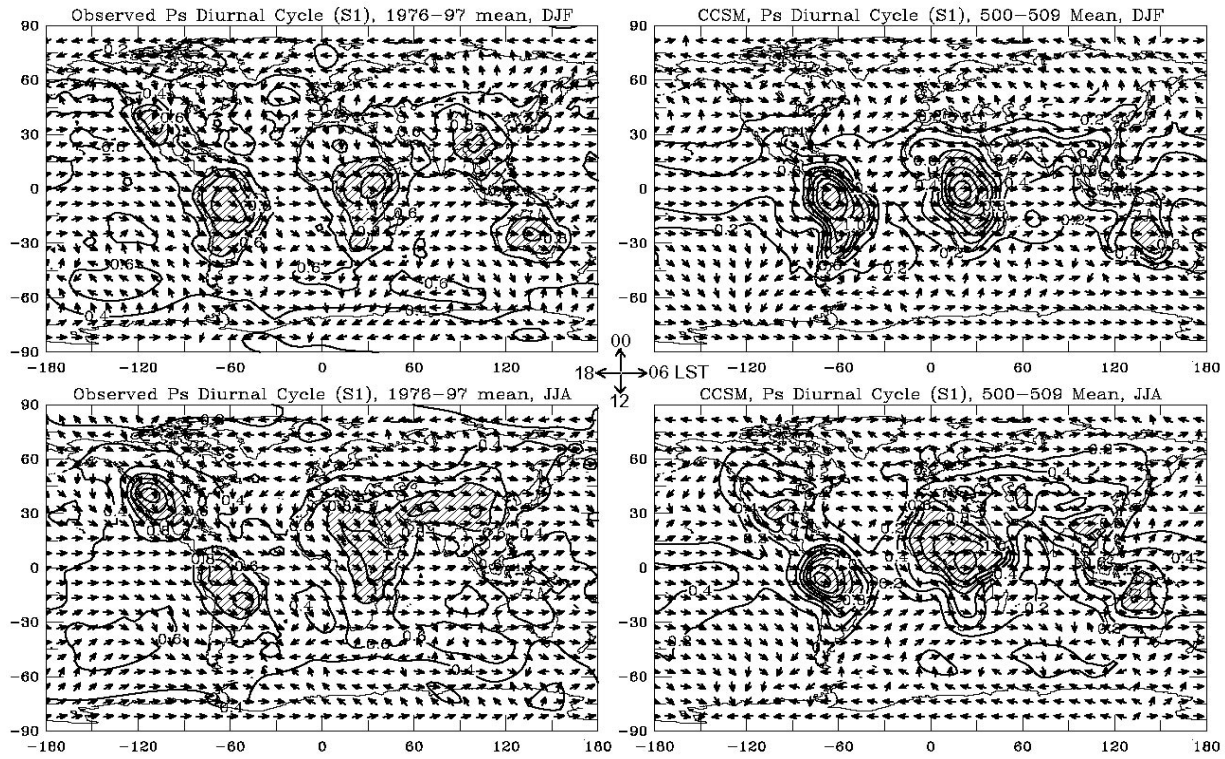


Fig. 4: Amplitude (contours, mb) and local solar time at the maximum (arrows, central phase clock) of the diurnal (24hr) harmonic of DJF (*top row*) and JJA (*bottom row*) surface pressure from observations (*left*, from Dai and Wang 1999) and the CCSM (*right*). Contour values over 8.0 mb are hatched.

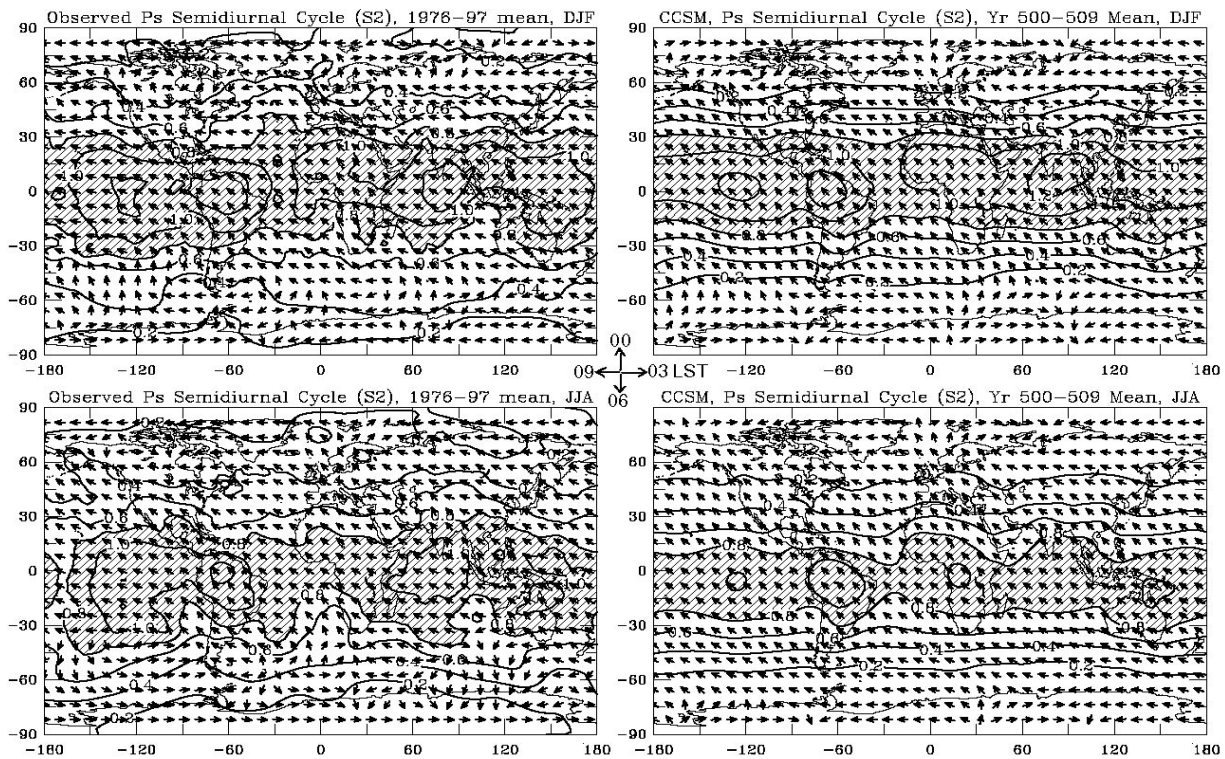


Fig. 5: Same as Fig. 4 but for the semidiurnal (12 hr) pressure tide. The phase is for the first peak.

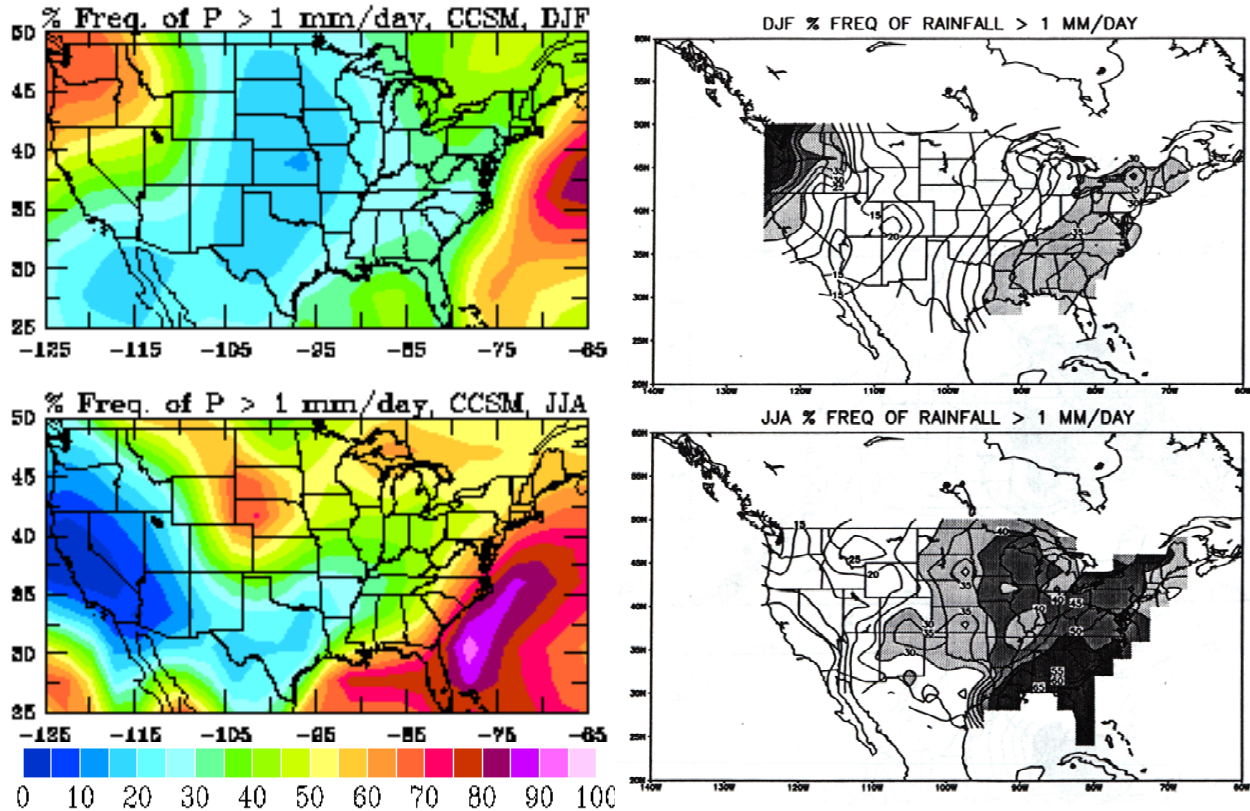


Fig. 6: CCSM-simulated (*left*, colors in %) and rain-gauge observed (*right*) DJF (*lower*) and JJA (*upper*) precipitation frequency (i.e. % of the total number of days with precipitation exceeding 1 mm/day) over the contiguous United States. The contour interval is 5% in right panels (from Higgins et al. 1996) and the shading indicates contour levels exceeding 30, 40, and 50% with increasing darkness.

Precipitation is a key climate variable that has many characteristics besides the amount. In order to simulate precipitation processes correctly, models need to simulate the right combination of frequency and intensity, not just the amount, of precipitation. Fig. 6 compares the CCSM-simulated percentage of the total number of days with precipitation exceeding 1 mm/day with that based on rain-gauge observations (Higgins et al. 1996) for the DJF and JJA seasons over the contiguous United States. The CCSM captures the general patterns and the magnitude of the frequency remarkably well. For example, the high frequency (exceeding 50%) in the Northwest, the low frequency (~10%) in the Central U.S., and the relatively high (30-35%) frequency in the East during DJF are simulated by the CCSM. The low frequency in the West and the high frequency in the East during JJA are also simulated, except that the model shows a local maximum frequency around the tri-state corner of Wyoming, Nebraska and South Dakota.

Fig. 7 compares the CCSM-simulated DJF and JJA precipitation frequency (same definition as in Fig. 6) to

that derived based on station and marine weather reports of non-drizzle precipitation (Dai 2001a). Many of the observed large-scale features are captured by the CCSM. For example, during DJF, the very high frequency (exceeding 70%) over the North Atlantic, North Pacific, and tropical Indian Ocean, and the very low frequency ($\leq 10\%$) over northern Africa, the Middle East, South Asia, and central America are reproduced by the model. During JJA, the very high frequency associated with the inter-tropical convergence zone (ITCZ) around 5-15°N from the central Pacific to central Africa and over the tropical Indian and western Pacific Ocean, as well as the very low frequency south of the Mediterranean Sea, in southern Africa, central and southern South America, and around the California coast, are also captured by the CCSM. Large discrepancies exist, however. For example, the simulated frequency is too low over much of Canada and Alaska in DJF, and over Europe and Russia in both DJF and JJA. The observed high DJF frequency band south of ~60°S is shifted northward by ~10° with a reduced magnitude in the CCSM.

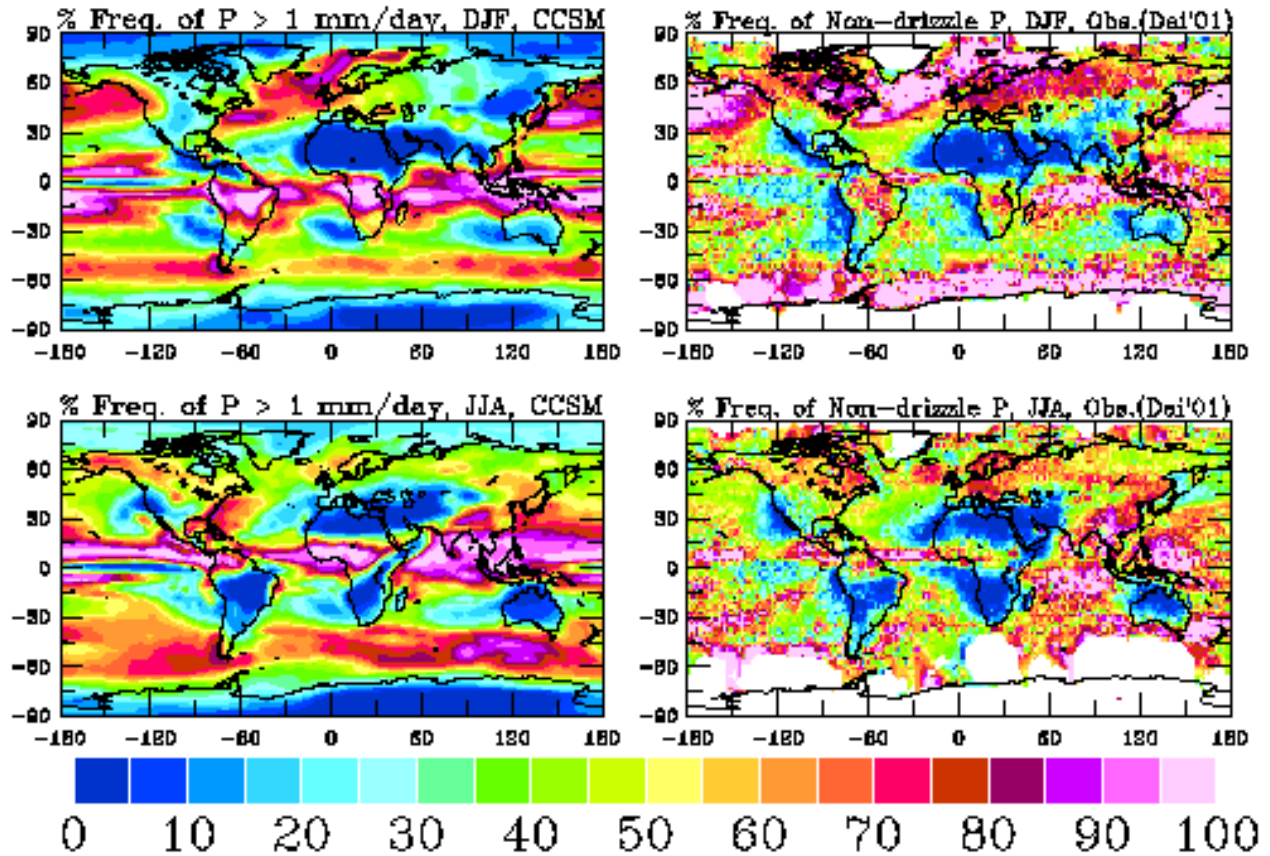


Fig. 7: CCSM-simulated (*left*, colors in %) and weather report-based (*right*) DJF (*lower*) and JJA (*upper*) precipitation frequency, i.e., the percentage of the total number of days with precipitation exceeding 1 mm/day in the CCSM or with one or more reports of non-drizzle precipitation for the right panels, which are from Dai (2001a).

Precipitation, especially summer convective rainfall, has pronounced diurnal cycles over most land areas and many oceans (e.g., Dai et al. 1999; Dai 2001b). Fig. 8 compares the local solar time of the maximum of the diurnal harmonic of convective precipitation in the CCSM with that of convective precipitation frequency derived from station and marine weather reports (see Dai 2001b for details). Since most of the diurnal variations of precipitation amount result from diurnal cycles in frequency not in intensity, the observed convective frequency diurnal cycle is a reasonable proxy for convective precipitation diurnal cycle. Fig. 8 shows that the simulated peak convective precipitation over land occurs around 1400-1600 LST, compared to 1600-1800 LST in the observations. Over many oceans such as the North Atlantic and North Pacific, the CCSM exhibits peak moist convection around 0200-0600 LST, versus 0400-0800 LST in the data. In addition, some regional features, such as the nocturnal maximum over the central United States, are not captured by the model. This is expected as the CCSM can not adequately resolve the Rockies and the low-level jet east to the

Rockies at a T42 ($\sim 2.8^\circ$) resolution. These phase biases suggest that peak moist convection tends to occur about 2 hrs too early in the CCSM. This premature-release of atmospheric convective available energy indicates that either the model's criterion for onset of moist convection is too weak or the diurnal cycle of low-level convergence/disturbance in the planetary boundary layer (PBL) is incorrect in the model.

Fig. 9 compares the diurnal amplitude (normalized by the daily mean) and phase of DJF and JJA convective precipitation in the CCSM with those of showery precipitation frequency derived from weather reports (Dai 2001b). The normalized diurnal amplitude is larger in the model (40-80% of the mean) than in the observations (30-70%) over northern midlatitude continents during JJA, but is too small over Africa and Australia during DJF. Over the oceans, the simulated amplitude is $\sim 10\%$, compared to the observed 20-60%. This, again, results largely from the lack of a diurnal cycle in the surface oceans in the CCSM.

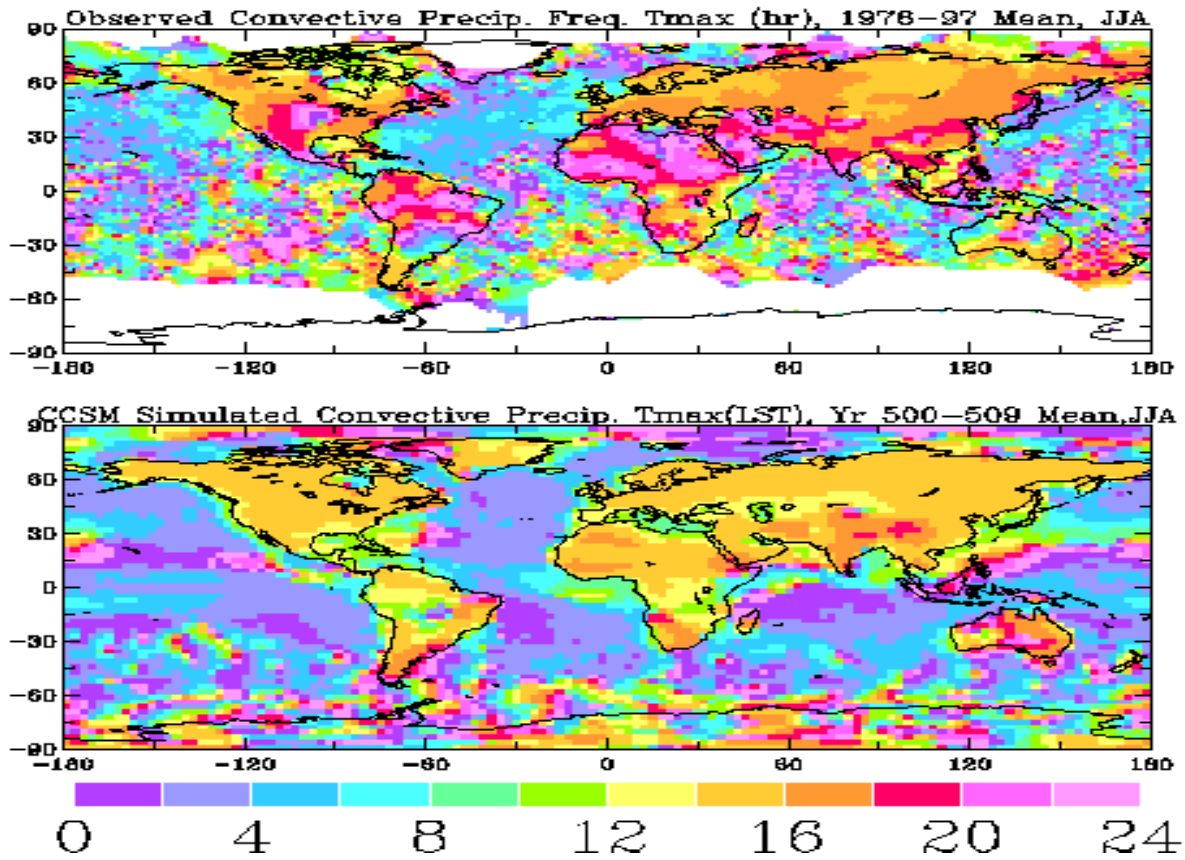


Fig. 8: The local solar time (hr) of the maximum of the diurnal harmonic of JJA convective precipitation frequency based on weather reports (*top*, from Dai 2001b) and of JJA convective precipitation in the CCSM (*bottom*).

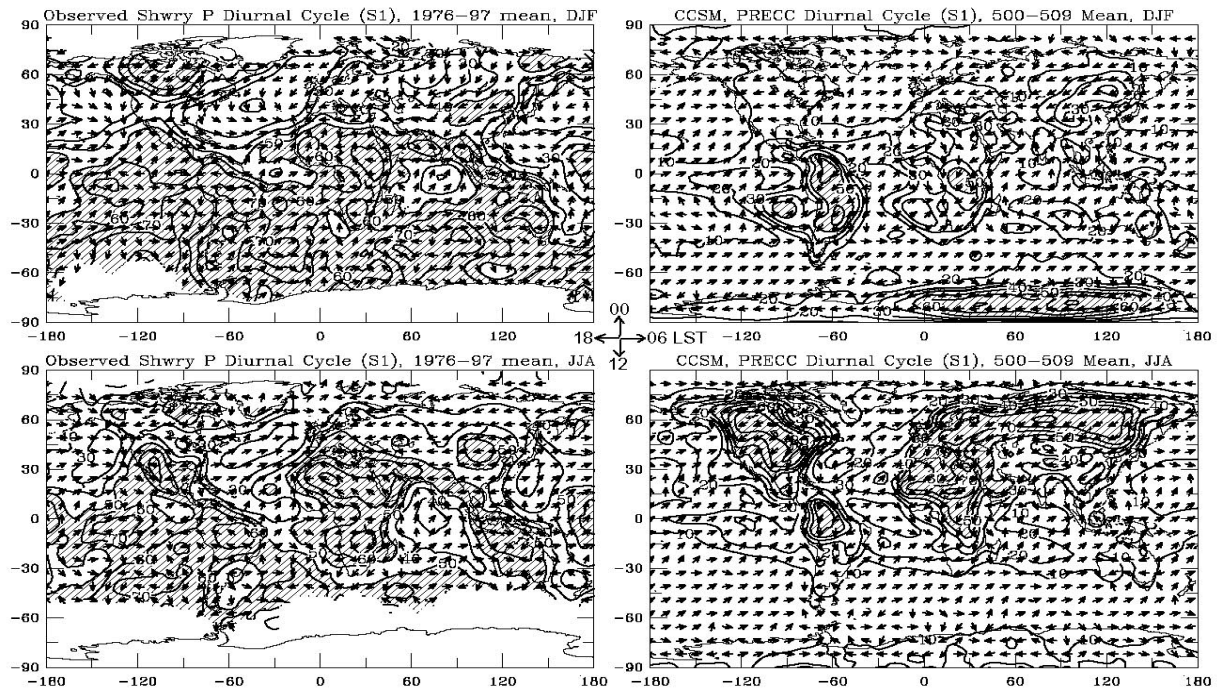


Fig. 9: Same as Fig. 2 but for observed showery precipitation frequency (*left*, from Dai 2001b) and CCSM-simulated convective precipitation (*right*). Contour values (in % of daily mean) over 50% are hatched.

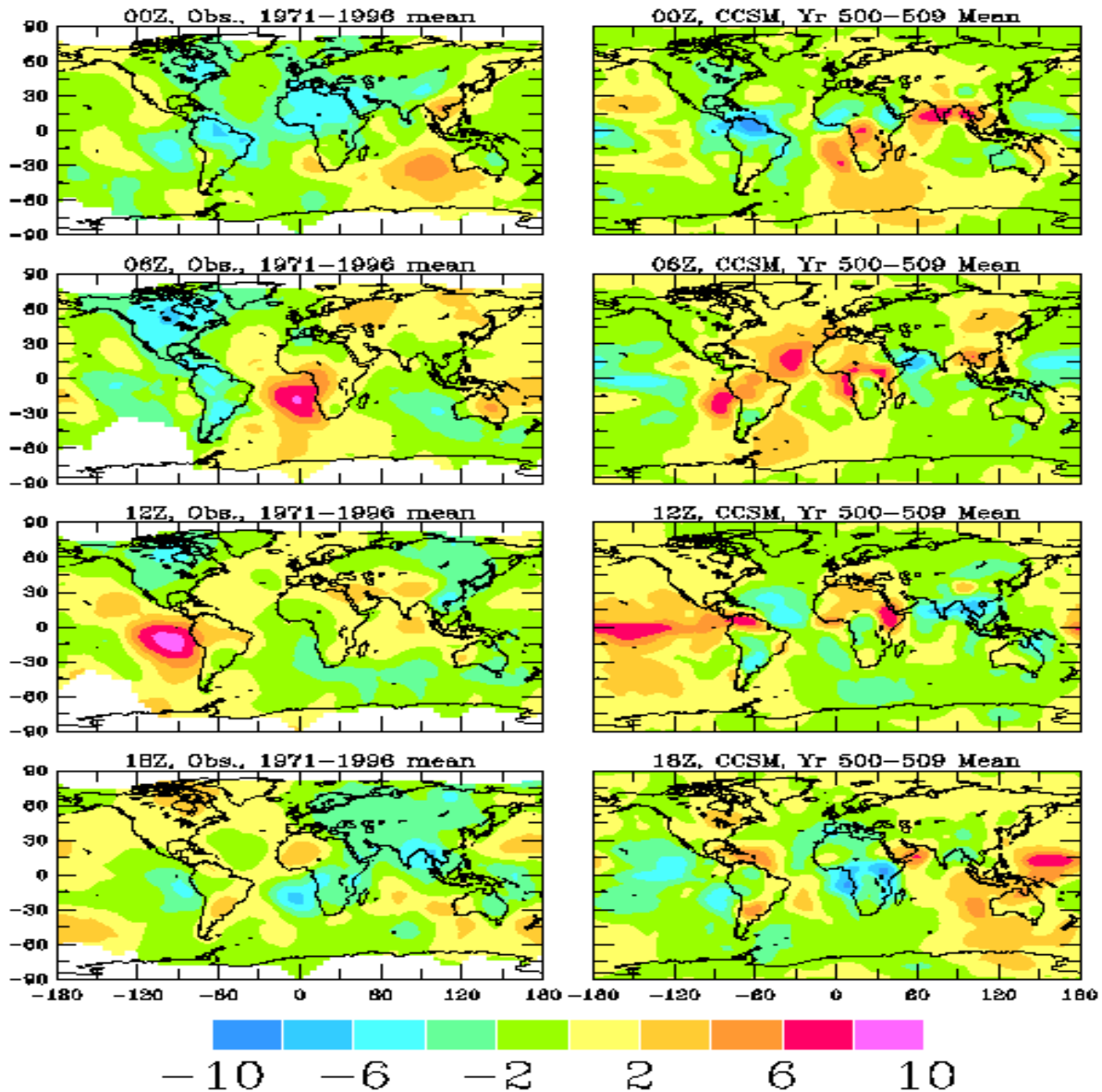


Fig. 10: Mean DJF diurnal anomalies of observed (*left*, from Hahn and Warren 1999) and CCSM-simulated (*right*) total cloud amount (in % of the sky dome) at 0000, 0600, 1200 and 1800 UTC.

A more challenging task for the model is to simulate the diurnal cycle of clouds, which greatly affect solar and infrared radiation. The surface observed total cloud cover (excluding dark-night conditions, from Hahn and Warren 1999) roughly shows a wave number 2 mode with peak cloud cover in the afternoon and early morning with many regional variations (Fig. 10). In the CCSM, a wave number 1 mode seems to be more evident (Fig.10). In particular, the diurnal cycle of subtropical marine stratus clouds west to North and South America and Africa is not simulated well by the CCSM. For example, the surface observations show peak stratus clouds around 1200 UTC west to South

America, but the model shows a reduced peak of stratus around 0600 UTC over the region. The strong diurnal cycle of stratus clouds west to Africa is also not simulated well. Plots of diurnal anomalies for low clouds (not shown) revealed patterns similar to Fig. 10, suggesting that diurnal variations in low clouds, such as stratus and cumulus clouds, dominate the diurnal cycle of total cloud cover. This is expected since these low clouds are strongly coupled with conditions at the surface and within the PBL where there is a pronounced diurnal cycle.

3. Summary

The CCSM reproduces the diurnal cycles of land surface air temperature and pressure, and the semidiurnal pressure tide over the globe; but it has too weak diurnal cycles for marine air temperature and pressure mainly because the sea surface temperature does not have a diurnal cycle in the model. Convective precipitation in model peaks around 2-4 pm in the afternoon over land and 2-6 am in the morning over ocean, which is ~2 hour too early over both land and ocean compared to observations. The normalized amplitude of the precipitation diurnal cycle is too strong over northern midlatitude continents during JJA, but too weak over the oceans. Diurnal variations of cloud cover, especially of marine stratus clouds, are not simulated well in the CCSM. Comparisons between simulated and NCEP/NCAR reanalysis upper air winds revealed remarkable agreements even regional scales. These results suggest that the surface energy balance over land and atmospheric solar absorption by ozone and water vapor seem to be represented well in the CCSM, whereas the diurnal cycle over the oceans and the simulations of clouds and precipitation need to be improved considerably.

References:

- Blackmon, M., et al., 2001: The Community Climate System Model. *Bull. Am. Met. Soc.*, **82**, 2357-2376.
- Chen, S.S. and Houze Jr, R. A., 1997: Diurnal variation and life-cycle of deep convective systems over the tropical Pacific warm pool. *Q. J. R. Meteorol. Soc.*, **123**, 357-388.
- Dai, A., 2001a: Global precipitation and thunderstorm frequencies. Part I: seasonal and interannual variations. *J. Climate*, **14**, 1092-1111.
- Dai, A., 2001b: Global precipitation and thunderstorm frequencies. Part II: diurnal variations. *J. Climate*, **14**, 1112-1128.
- Dai, A. and J. Wang, 1999: Diurnal and semidiurnal tides in global surface pressure fields. *J. Atmos. Sci.*, **56**, 3874-3891.
- Dai, A., F. Giorgi, and K.E. Trenberth, 1999: Observed and model simulated precipitation diurnal cycle over the contiguous United States. *J. Geophys. Res.*, **104**, 6377-6402.
- Hahn, C.J. and S.G. Warren, 1999: Extended edited synoptic cloud reports from ships and land stations over the globe, 1952-1996. ORNL/CDIAC-123, NDP-026C, 71 pp.

- Higgins, R.W., J.E. Janowiak, and Y.-P. Yao, 1996: A gridded hourly precipitation data base for the United States (1963-1993), *NCEP/Climate Prediction Center ATLAS No. 1*, U.S. Dept. of Commerce, Washington, D.C., 47 pp.
- Kent, E.C., R.J. Riddy and P.K. Taylor, 1993: Correction of marine air temperature observations for solar radiation effects. *J. Atmos. & Oceanic Tech.*, **10**, 900-906.
- Sui, C.-H., K.-M. Lau, Y.N. Takayabu, and D.A. Short, 1997: Diurnal variations in tropical oceanic cumulus convection during TOGA COARE. *J. Atmos. Sci.*, **54**, 639-655.
- Zeng, X., Q. Zhang, D. Johnson, and W.-K. Tao, 2002: Parameterization of wind gustiness for the computation of ocean surface fluxes at different spatial scales. *Mon. Wea. Rev.*, **130**, 2125-2133.